

# Mechanical modelling of Alkali-Aggregate Reaction in concrete structures

B.Capra & A.Sellier

Laboratoire de Génie Civil et Urbanisme 2, rue A. Einstein - Cité Descartes 77420 Champs-sur-Marne, France

**ABSTRACT:** Alkali-Aggregate Reaction (AAR) is difficult to model due to the random distribution of the reactive sites and the imperfect knowledge of these chemical reactions. A new approach, based on a probabilistic description of the main physical parameters of concrete and AAR, allows to simulate anisotropic swelling of concrete subjected to AAR. The concrete is modelled like a damageable material having elastic and inelastic strains. AAR is modelled by a global kinetics including temperature and humidity effects. The coupling between mechanics and AAR makes it possible to simulate tests carried out on concrete specimens. The results, obtained in terms of axial and transverse strains versus time, for various levels of axial loading, show a good agreement between experimental results and model response.

## 1 INTRODUCTION

A lot of structures, such as dams or bridges, are suffering from deteriorations induced by Alkali-Aggregate Reaction (AAR) that impair durability and might also affect the safety of installations. AAR induces concrete expansion and generally leads to loss of strength and cracking. There is an increasing interest in the structural response to AAR effects. Need for, and nature of potential intervention must be supported by knowledge of the spatial distribution and intensity of swelling, stress state resulting from it, and long term evaluation of the swelling process.

Such a reaction is difficult to model accurately because of the complexity of the phenomena : random localisation of the reactive sites, imperfect knowledge of the reaction mechanisms, etc. In order to perform structural computations, reactions have been modelled within a phenomenological approach framework by taking into account the following major parameters : the kinetic of the reaction, the temperature, the moisture and the stress state. These variables will then govern the raising pressure which represents the mechanical effects of the reactions within concrete. Furthermore, concrete modelling is based on a physical description of the crack opening probability. This probability is related to the damage rate of the material. The constitutive model allows then to describe an anisotropic decreasing of the elastic properties of concrete and the residual

swelling, under both AAR and mechanical loads. Numerical simulations have been performed to compare the model response to the experimental results of tests carried out at the Laboratoire Central des Ponts et Chaussées. The behaviour of specimens subjected to different uniaxial loads has been properly reproduce in terms of residual strains and anisotropic swelling.

## 2 MECHANICAL MODELLING OF CONCRETE

### 2.1 Effective Stresses – Elastic Strains Relations

The elastic part of the behaviour law of concrete is based on orthotropic damage theory (Lemaitre & Chaboche 1988). The elastic strains are calculated from the effective stresses as follows (Sellier et al. 1998) :

$$\left\{ \begin{array}{l} \varepsilon_i^e = \frac{1}{E_i^+} \sigma_{eff}^+ + \frac{1}{E_0} \sigma_{eff}^- - \frac{\nu_0}{E_0} (\sigma_{eff}^+ + \sigma_{eff}^-) \\ \text{with : } \frac{1}{E_i^+} = \frac{1}{E_0} (P_i + (1 - P_i) \left( \frac{1 - d_i^+}{1 - d_i^{*+}} \right)) \\ \sigma_{appi} = \sigma_{eff}^+ (1 - d_i^+) + \sigma_{eff}^- (1 - d_i^-) \end{array} \right. \quad (1)$$

In these expressions, the sign “+” or “-” denotes the sign of the principal effective stress (“+” for

compression, “-“ for tension). The indices  $i, j$  and  $k$  represent the three cartesian directions.  $\varepsilon_i^e$  is the elastic strain,  $\sigma_{appi}$  and  $\sigma_{effi}$  are the apparent and effective stress respectively. As the law is orthotropic, the damages coefficients  $d_i$  may be calculated for any direction among the three principal directions in the stress operating space.  $E_0$  and  $\nu_0$  are respectively the Young modulus and the Poisson ratio for the initial and undamaged material.  $P_i = l_c / l_i$  where  $l_c$  is an internal length considered in order to avoid the numerical strain localisation problem and  $l_i$  is the element dimension in the “ $i$ ” direction follows (Sellier et al. 1998). These coefficients act on the post-peak part of the behaviour law by imposing an energy dissipation independent of the characteristic size of the element calculated in direction “ $i$ ” (Barzegar & Maddipudi 1997).  $d_i^* = \min(d_i, d_i^{peak})$  where  $d_i^{peak}$  is the damage at the peak of the behaviour law, represented by the curve stress versus strain. The expression of elastic strain assumed that energetic dissipation is volumic until the peak and is surfacic after the peak, in accordance with experimental results (Jansen & Shah 1997). The guiding principles of mechanical modelling being posed, we now will study the modelling of AAR before establishing the coupling by the use of the damage coefficients.

### 3 MODELLING OF AAR

#### 3.1 Self-Stresses Generated by AAR

The following figure schematically represents the state of stress of concrete subjected to AAR :

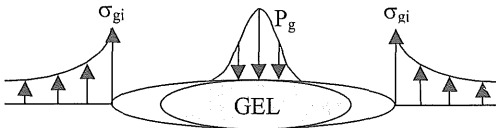


Figure 1 : Self-stresses generated by AAR.

The self-stress generated by AAR, in the direction “ $i$ ”, on uncracked concrete (fraction  $1 - Pf_{aari}$ ) must balance the pressures generated in the cracks filled with products of reaction. Let  $P_g$  be the average pressure exerted by those products on the cementitious matrix, and  $\sigma_{gi}$  the stress induced on the undamaged material. The equilibrium equation leads to the following relation, valid for the three principal directions “ $i$ ” :

$$\sigma_{gi} = -\frac{P_g}{(1 - Pf_{aari})} \quad (2)$$

$Pf_{aari}$  represents the probability of cracking due to AAR in direction “ $i$ ”.  $(1 - Pf_{aari})$  is thus the fraction of uncracked material, in direction “ $i$ ”, on which  $\sigma_{gi}$  is exerted.

#### 3.2 Gel Pressure

The pressure generated in the gel ( $P_g$ ) is proportional to the volume of gel created and its rate of confinement. Let  $V_g$  be the volume of gel created during the reactions,  $V_{eaar}$  the volume of the cracks occupied by the gel,  $V_{p0}$  the volume of porosity connected to the reactive sites likely to be used as an expansion vessel for gel. The pressure developed by the reactions is expressed by :

$$P_g = K \left( V_g - V_{p0} - V_{eaar} \right)^+ \quad (3)$$

where :  $\langle X \rangle^+ = X$  if  $X > 0$   
 $= 0$  if  $X < 0$

The volume of the cracks occupied by AAR ( $V_{eaar}$ ) is supposed to be proportional ( $k_e$ ) to the total volume of created cracks (related to the cubic dilatation  $tr\varepsilon$ ), to the quantity of gel likely to penetrate there ( $V_g$ ) and to the pressure  $P_g$  which will allow the gel penetration in these cracks :

$$V_{eaar} = k_e \cdot P_g \cdot V_g \cdot tr\varepsilon \quad (4)$$

Porous volume accessible to AAR ( $V_{p0}$ ) is supposed to be proportional to the initial porosity of the concrete ( $P_0$ ) :

$$V_{p0} = k_p \cdot P_g \cdot V_g \cdot P_0 \quad (5)$$

These expressions make it possible to express the gel pressure by:

$$P_g = K \left( \frac{V_g}{1 + K \cdot V_g (k_e \cdot tr\varepsilon + k_p \cdot P_0)} \right)^+ \quad (6)$$

where  $K$  is a stiffness constant of gel, to be determined by inverse analysis.

#### 3.3 AAR Global Kinetics

AAR global kinetics stands for  $[Na_2O_{eq}]$  total concentration of the pore solution in alkaline Sodium equivalent ( $Na_2O + 0.658 \cdot K_2O$ ). Let us

regard this concentration as the chemical tracer of AAR and suppose that the following reaction represents the consumption of alkalis by AAR (Capra 1997) :



If A(t) is the percentage of reacted alkalis during time t :

$$A(t) = \frac{[\text{Na}_2\text{O}_{\text{eq}}](0) - [\text{Na}_2\text{O}_{\text{eq}}](t)}{[\text{Na}_2\text{O}_{\text{eq}}](0)} \quad (7)$$

It is supposed that the volume of gel created during time t is proportional to the percentage of reacted alkalis. By making the assumption that first order kinetics is representative of the reactions, and that an Arrhenius law can apply to AAR, one obtains the following form for the gel pressure  $P_g(t)$  (Capra et al. 2000) :

$$P_g(t) = K \left\langle \frac{P_{g \text{ lim}}(t)}{1 + P_{g \text{ lim}}(t) \cdot (k_e \cdot t \cdot \varepsilon + k_p \cdot P_0)} \right\rangle^+ \quad (8)$$

where :

$$P_{g \text{ lim}}(t) = P_{g \text{ lim}}^\infty \cdot \text{RH}^m \cdot \left( 1 - \exp\left(-k_0 \cdot \exp\left(-\frac{E_a}{RT}\right) t\right) \right) \quad (9)$$

The effects of the relative humidity (RH) on AAR are introduced in a global way by a reducing function ( $\text{RH}^m$ ) of the gel pressure.  $P_{g \text{ lim}}^\infty$  is the maximum gel pressure which can be reached in the concrete at an infinite time and for a saturated relative humidity ( $\text{RH}=100\%$ ).  $E_a$  is the activation energy of the reaction, T the absolute temperature,  $k_0$  a global kinetic constant of the chemical processes related to the reactions.

### 3.4 Probability of Cracking Related to AAR

The auto-stress  $\sigma_{gi}$ , generated by AAR, is superimposed locally on the stresses due to a mechanical loading of the concrete,  $\sigma_i$ . The probability of cracking due to AAR, in the principal direction "i",  $Pf_i^{\text{AAR}}$ , then reads to :

$$Pf_i^{\text{AAR}} = 1 - \exp\left(-\frac{1}{m_r} \left\langle \frac{\langle \sigma_i + \sigma_{si} \rangle^+}{\sigma_i^{\text{ur}}} \right\rangle^{m_r}\right) \quad (10)$$

The choice of a Weibull's law for  $Pf_i^{\text{AAR}}$  is more

detailed in (Sellier et al. 1999).  $\sigma_i^{\text{ur}}$  is the cohesion of Weibull, in the direction "i";  $m_r$  is the exponent of Weibull, supposed homogeneous and isotropic.

### 3.5 Probability of Cracking Due to Tensile and Compressive Stresses

In a way identical to the probability of cracking due to AAR, one can define a probability of cracking due to a mechanical loading of tension ( $Pf_i^t$ ) or compression ( $Pf_i^c$ ). The following relations express the fact that the cracks from mechanical origin can have two sources : direct and indirect. A tensile stress has a direct effect on the opening of a crack in the loading direction. On the other hand, a compressive stress generates self-stresses of traction perpendicular to the loading direction which will crack the concrete. The preceding remarks lead to the following equations :

$$Pf_i^t = 1 - \exp\left(-\frac{1}{m^+} \left\langle \frac{\langle \sigma_i \rangle^+}{\sigma_i^{\text{ur}}} \right\rangle^{m^+}\right) \quad (11)(12)$$

$$Pf_i^c = 1 - \exp\left(-\frac{1}{m^-} \left\langle \frac{\langle \sigma_i + \sqrt{(C^-)^2 \left( \langle \sigma_j \rangle^- \right)^2 + \langle \sigma_k \rangle^- \right)^2}{\sigma_i^{\text{ur}}} \right\rangle^{m^-}\right)$$

$\sigma_i^{\text{ur}}$ ,  $\sigma_i^{\text{ur}c}$  are the Weibull's cohesions in direct tension and in indirect tension (perpendicular compression) respectively.  $C^-$  is the coefficient of variation in compression.  $m^+$ ,  $m^-$  are the exponents of Weibull in tension and compression respectively.

## 4 DAMAGE OF CONCRETE : COUPLING AAR / MECHANICS

### 4.1 Damage Coefficients

The damage coefficients in tension  $d_i^+$  and in compression  $d_i^-$  used in equation (1) are calculated according to the probabilities of cracking in the following way :

$$\begin{aligned} d_i^+ &= 1 - (1 - Pf_i^t)(1 - Pf_i^c)(1 - Pf_i^{\text{AAR}}) \quad (13)(14) \\ d_i^- &= 1 - (1 - Pf_i^c)^{\nu(L)} \cdot (1 - Pf_i^t)^{\nu(L)} \cdot (1 - Pf_i^{\text{AAR}})^{\nu(L)} \\ &\quad \cdot (1 - Pf_i^c)^{\nu(k)} \cdot (1 - Pf_i^t)^{\nu(k)} \cdot (1 - Pf_i^{\text{AAR}})^{\nu(k)} \end{aligned}$$

These damage coefficients are deduced from the different probabilities previously calculated

according to the weakest link theory. These coefficients express the various sources of damage : direct and indirect tension, damage due to AAR. The weighing functions  $\psi$  allow possible crack reclosing in case of cyclic loadings.

#### 4.2 Total Strains

The total strains  $\varepsilon_i$  are supposed to be the sum of the elastic strain  $\varepsilon_i^e$ , the mechanical anelastic strains

$\varepsilon_i^{pl}$  (without AAR) and of the strains due to AAR

$$\varepsilon_i^{AAR} : \varepsilon_i = \varepsilon_i^e + \varepsilon_i^{pl} + \varepsilon_i^{AAR} \quad (15)$$

We assume that the mechanical anelastic strains are independent of AAR. The relations between elastic strains and effective stresses have been detailed in equation (1). An example of the apparent stress /elastic strain relationship is presented by the following figure :

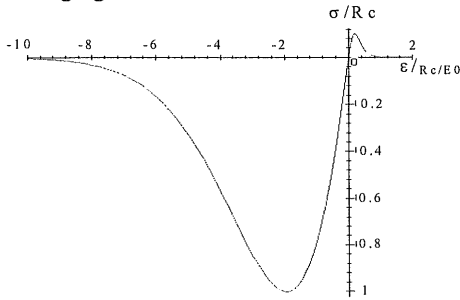


Figure 2 : Stress – elastic strain curve obtained in uniaxial loading path ( $m=1.5$ ,  $C=0.5$ ,  $\sigma_u=2.03$ MPa,  $C^+=6.94$ ,  $E_0=30000$  MPa,  $\nu_0=0.2$ ,  $R_c=25$  MPa : compressive strength of concrete).

#### 4.3 Anelastic Strains Due to AAR

The anelastic opening of the cracks due to AAR evolves in an asymptotic way when cracking becomes significant, this phenomenon is modelled by the following equation :

$$\varepsilon_i^{AAR} = \varepsilon_0^{AAR} \frac{Pf_i^{AAR}}{1 - Pf_i^{AAR}} \quad (16)$$

where  $\varepsilon_0^{AAR}$  is a material parameter to be determined. The use of the relations between probability of cracking and damage on the one hand, probabilities of cracking and swelling on the other hand, makes it possible to link AAR swelling and damage :

$$\varepsilon_i^{AAR} = \varepsilon_0^{AAR} \frac{d_i^+}{1 - d_i^+} \quad (17)$$

Experimental results (ISE 1992, Larive 1997) show a decrease of the mechanical characteristics of concrete according to the swelling rate. The figure 3 presents the experimental data used to determine  $\varepsilon_0^{AAR}$  by the use of equation (17). The fitting leads to :

$$\varepsilon_0^{AAR} = 0.3 \% \quad (18)$$

This parameter seems to be relatively constant even for tests carried out on different concrete mixes.

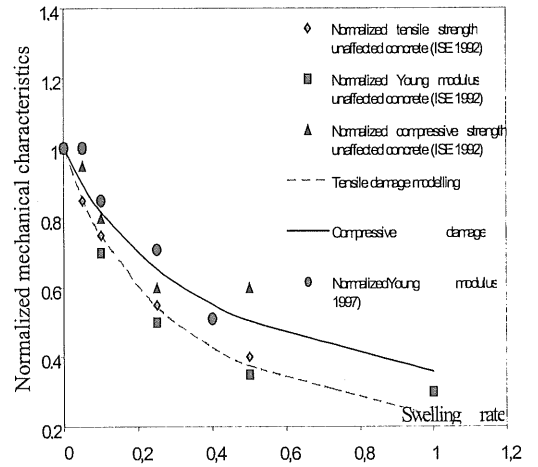


Figure 3 : Evolution of the mechanical characteristics versus AAR swelling rate.

#### 4.4 Anelastic Strains of Mechanical Origin

In this section, we assume that the anelastic strains of mechanical origin are expressed by :

$$\varepsilon_i^{pl} = \varepsilon_i^+ + \varepsilon_i^- \quad (19)$$

Indice “+” and “-” stands for compression and tension respectively. As for elastic behaviour, probabilities of cracking are introduced, leading to the following expressions of the anelastic strains :

$$\varepsilon_i^+ = \varepsilon_0^+ \cdot P_i \cdot \psi_i \cdot \frac{Pf_i^+ - Pf_i^{*+}}{1 - Pf_i^+} \quad (20)(21)$$

$$\varepsilon_i^- = \varepsilon_0^- \left( \frac{Pf_i^-}{1 - Pf_i^-} \psi_i - \nu_p \left( \frac{Pf_j^-}{1 - Pf_j^-} \psi_j + \frac{Pf_k^-}{1 - Pf_k^-} k \psi_k \right) \right)$$

The signification of the various terms is not described here but the reader will find more details in (Sellier et al. 1999). The following figures compare experimental results and numerical simulations of biaxial behaviour of concrete subjected to an uniaxial loading :

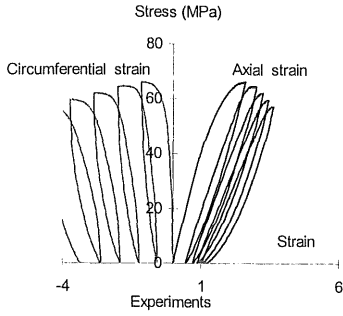


Figure 4 : Experimental results of the behaviour of concrete in pure compression

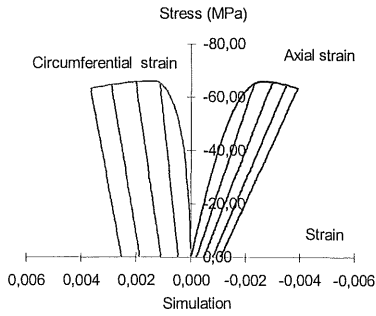


Figure 5 : Numerical simulations of the behaviour of concrete in pure compression

5 NUMERICAL SIMULATIONS OF AAR

5.1 Swelling under uniaxial loading

Tests of swelling under uniaxial loading, with measurements of axial and transverse strains, were carried out at the Laboratoire Central des Ponts et Chaussées (Larive 1997). The model presented previously was applied to these tests. The following figures present the response of the model compared with the experimental points for various loadings : free swelling, 5, 10 and 20 MPa of compression. The model shows a good agreement with the tests except for transverse swelling under 10 MPa. The model is able to reproduce tridimensionnal swelling of concrete under various loading cases.

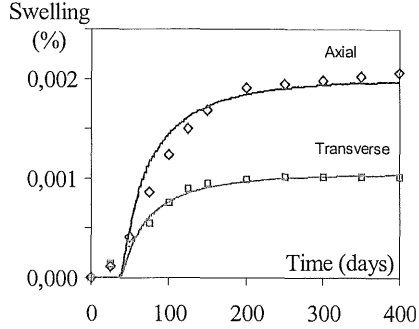
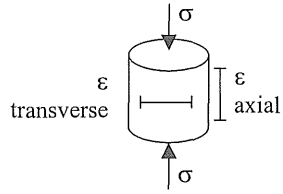


Figure 6 : Comparison between experimental points and numerical modelling (free swelling :  $\sigma=0$  Mpa).

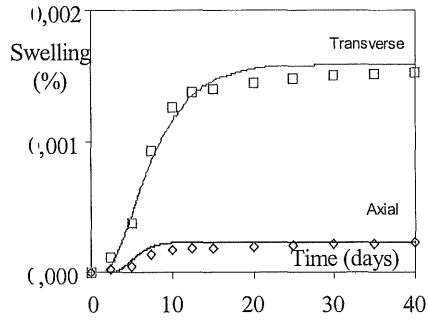


Figure 7 : Comparison between experimental points and numerical modelling (compressive loading : 5 Mpa).

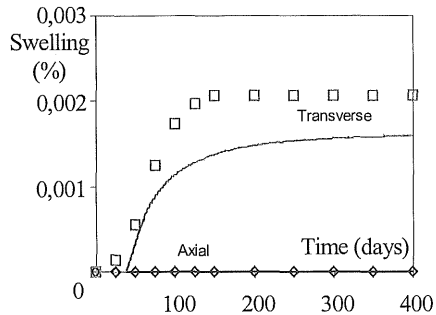


Figure 8 : Comparison between experimental points and numerical modelling (compressive loading : 10 Mpa).

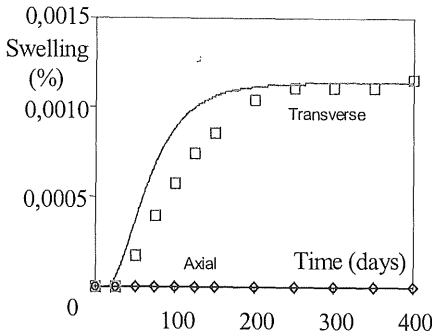


Figure 9 : Comparison between experimental points and numerical modelling (compressive loading : 20 Mpa).

### 5.2 Numerical simulation of a beam subjected to AAR

The previous model of concrete subjected to internal swelling has been implemented in the finite element code CASTEM 2000 developed by the CEA (Commissariat à l’Energie Atomique). In order to test the model, the following example has been computed :

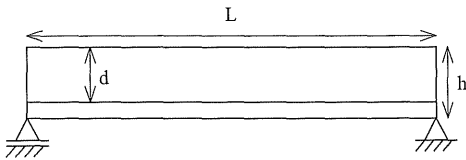


Figure 9 : Re-enforced beam subjected to AAR.

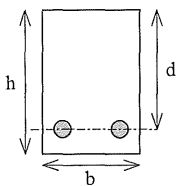


Figure 10 : Typical cross-section of the beam.

The parameters of the problem are the following ones :

$$L = 3\text{ m}$$

$$h = 0.5\text{ m}$$

$$b = 0.25\text{ m}$$

$$d = 0.45\text{ m}$$

$$\text{Re-enforcement : } 2 \text{ HA } 25 = 9.81\text{ cm}^2$$

The principal parameters of the behaviour of the materials are :

Steel bars : Elastic behaviour

$$\text{Young's modulus : } E_s = 210000\text{ MPa}$$

$$\text{Poisson's coefficient : } \nu_s = 0.3$$

$$\text{Volumetric mass : } \rho_s = 7850\text{ kg/m}^3$$

Concrete: Non linear orthotropic damageable behaviour

Initial Young's modulus :

$$E_c = 42000\text{ Mpa}$$

$$\text{Poisson's coefficient : } \nu_c = 0.2$$

$$\text{Volumetric mass : } \rho_c = 2500\text{ kg/m}^3$$

The dead-weight of concrete is taken into account. The beam is subjected to no external mechanical loading, except the dead-weight. The concrete of the beam is subjected to AAR. The figure 11 shows the evolution of the pressure developed by the gel created versus time, following equation 9. Numerical values have been estimated using experimental tests carried out by Larive (Larive 1997) :

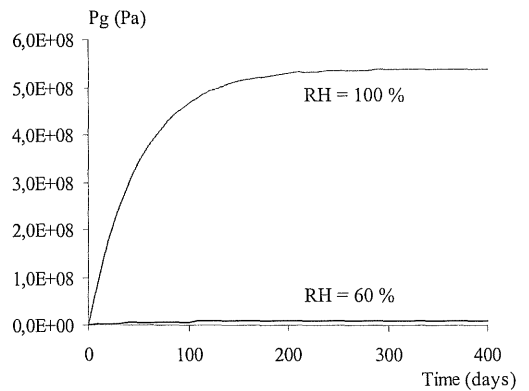


Figure 11 : Evolution of the gel pressure versus time for different relative humidity (RH) of concrete.

At the moment, there are few studies concerning the effects of the relative humidity on the swelling due to AAR. Nevertheless, it is well known that under a relative humidity of 50 or 60 % in concrete, there is no more swelling. In order to model these observations, the exponent  $m$  in equation 9 is taken equal to 8, which provide a fast diminution of pressure when RH decrease.

The following figure shows the gradient of humidity that have been applied to the beam :

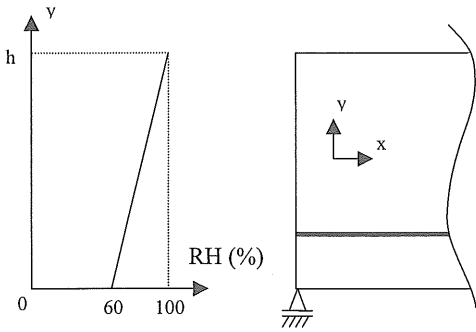


Figure 12 : Gradient of humidity applied to the beam (top : 100%, bottom : 60 %).

The finite element mesh used for the simulations in plane stresses of the half-beam and the boundary conditions are represented on the following figure :

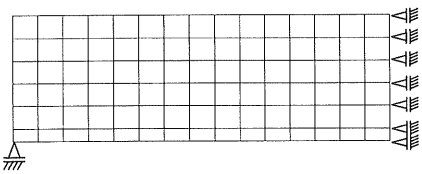
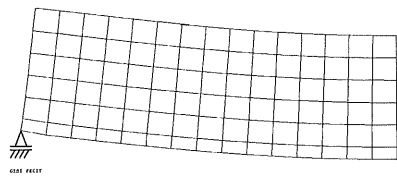
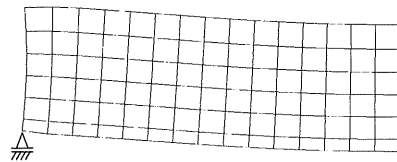


Figure 13 : Finite element mesh and boundary conditions.

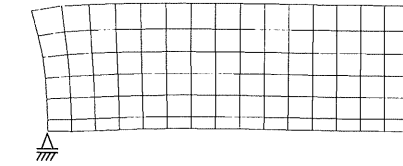
The following figures show the deformed mesh of the beam for different time :



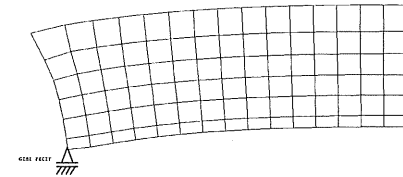
t = 0 : deformed mesh under dead-weight



t = 40 days



t = 80 days



t = 200 days

Figure 14 : Evolution of the deformed shape of the beam during time.

The previous figures show that the gradient of humidity, i.e. the gradient of swelling, is able to change the curvature of the beam. Such a phenomenon is often observed on real structures and reproduce in laboratory (Swamy & Al-Asali 1989). During the same time, even if the curvature has changed, the bottom of the beam is still in tension. There is even a tension increase inside the bars which can lead, sometimes, to the break it on real structures. The following figures show the evolution of the damage coefficients  $d_{xx}$  and  $d_{yy}$  due to AAR on the beam :

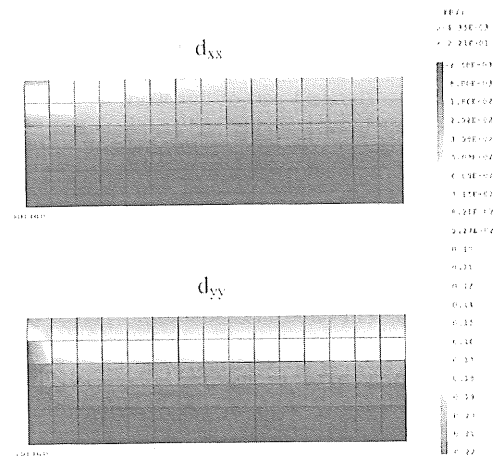


Figure 15 : Damage fields due to AAR

The more damage part of the beam is on the top left corner because there is the maximum of humidity, like all the top fiber of the beam, but also no

confinement by the surrounding material. The damage is preferentially located in the first row of element because the decrease of humidity, i.e. swelling, is very fast. Furthermore, for the level of gel pressure used, the compression at the top of the beam implies  $d_y$  as the major damage. Further simulations need to be performed in order to take into account the effect of a temperature field coupled with a gradient of humidity and higher gel pressure.

## 6 CONCLUSION

The three-dimensional modelling of AAR presented here makes it possible to perform mechanical / chemistry coupled simulations. It requires, on the one hand, a powerful behaviour law of the concrete capable to represent the anisotropic behaviour of the material in terms of strains and damage. In addition, this modelling of AAR is based on a global description of the chemical kinetics of the reactions and on a physical description of the swelling mechanisms. The method employed to take into account the coupling between chemical and mechanical phenomena leads to a model which integrates the various possible sources of concrete damage. The numerical simulations performed show a good agreement between experiments and the model responses. These results highlight the need for having a realistic description of the various physical mechanisms concerned in order to obtain a coherent response of the model. The numerical implementation of this model in a finite element code has been done. The first simulation of a beam subjected to AAR show some interesting results which reproduce some phenomenon observed on real structures. The next part of this work will be to determine if the loss of rigidity and bending capacity are in a good agreement with experiments.

## ACKNOWLEDGEMENTS

EDF-CIH is gratefully acknowledged for its financial support towards these studies.

## REFERENCES

Barzegar, F & Maddipudi, S. 1997. Three dimensional modelling of concrete structure I : plain concrete. *Journal Of Structural Engineering* 23 (10) : 1339-1346.  
 Capra, B. 1997. Modélisation des effets mécaniques induits par les Réactions Alcalis-Granulats, *PhD Thesis*, ENS Cachan.

Capra, B., Sellier, A. & Bourdarot, E. 2000. Mechanical modelling of Alkali-Aggregate Reaction in concrete. 11<sup>th</sup> Int. Conf. On Alkali-Aggregate Reaction, Québec, 11-16 June 2000. Dérubé, Fournier, Durand editors.  
 Institution of Structural Engineers, 1992. Structural effects of alkali-silica reaction, technical guidance on the appraisal of existing structures, Published by the Institution of Structural Engineers, London, July 1992.  
 Jansen, D.C. & Shah S.P. 1997. *Effect of length on compressive strain softening of concrete*. *Journal Of Engineering Mechanics*, 25 (1) : 25-35.  
 Lemaitre, J & Chaboche, J.L. 1988. *Mécanique des matériaux solides*. Paris : Dunod.  
 Larive, C. 1997. Apport combinés de l'expérimentation et de la modélisation à la compréhension de l'alcali-réaction et ses effets mécaniques, *PhD Thesis*, LCPC Paris.  
 Sellier, A., Capra, B. & Mébarki, A. 1998. Modélisation de la loi de comportement du béton : approche probabiliste. 2<sup>nd</sup> Conférence JN-FIAB '98, Marne-la-Vallée, 23-24 Novembre 1998 : 247-256.  
 Sellier, A., Capra, B. & Mébarki, A. 1999. Concrete behavior : a probabilistic damage model. 8<sup>th</sup> Int. Conf. Applications of Statistics and Probability, Sydney, 12-15 December 1999. Rotterdam : Balkema.  
 Swamy, R.N., Al-Asali, M.M. 1989. Effect of Alkali-Silica Reaction on the structural behavior of reinforced concrete beams. *ACI Structural Journal*, 86 (4) : 451-459.